

Energy dependence of the ${}^7\text{Li}(p,d){}^6\text{Li}$ reaction

J. J. Kraushaar, P. D. Kunz, and J. H. Mitchell

*Nuclear Physics Laboratory, Department of Physics, University of Colorado, Boulder, Colorado 80309*J. M. Cameron, D. A. Hutcheon, R. P. Liljestrand,* W. J. McDonald,
C. A. Miller, and W. C. Olsen*Department of Physics, University of Alberta, Edmonton, Alberta, Canada T6G 2N5*J. R. Tinsley[†]*Department of Physics, University of Oregon, Eugene, Oregon 97403*

C. E. Stronach

*Department of Physics, Virginia State University,
Petersburg, Virginia 23803*

(Received 2 May 1985)

Angular distributions for the transitions to the 1^+ ground state and 3^+ first excited state of ${}^6\text{Li}$ for the ${}^7\text{Li}(p,d)$ reaction have been obtained at 200 and 400 MeV. It has been shown that the ratio for the excitation of the 3^+ states relative to the 1^+ state can be accounted for at bombarding energies ranging from 16 to 800 MeV by the addition of a small amount of $1f_{7/2}$ in the wave function for the transition to the 3^+ states.

The ${}^7\text{Li}(p,d)$ reaction has been studied at various laboratories with incident protons that have ranged in energy from 16.7 to 800 MeV. Such an extensive set of cross sectional data permits one to examine the validity of the reaction mechanism on one hand, and to examine high momentum components of the wave function on the other. Stripping particles into nonzero spin nuclei raises the possibility of multiple l transfers. At the lower bombarding energies the low angular momentum transfers dominate, while at the higher energies the high angular momentum transfers are favored. Thus it is possible to distinguish between these different parts of the wave function for the transferred particle. Since the ${}^7\text{Li}$ nucleus can be described by the collective model with a deformation parameter β , near unity, there can be appreciable admixture of f states into the usual p -shell description of the transferred nucleon.

It has been noticed previously that the ratio of the cross sections for the 3^+ first excited state of ${}^6\text{Li}$ to the 1^+

ground state, both $l=1$ transitions, appeared to increase rather dramatically as the energy was increased. Data are available on the (p,d) reaction to these two states at 16.7,¹ 33.6,² 100,³ 156,⁴ 185,⁵ and 800 MeV (Ref. 6). In order to have a more complete set of data, particularly at intermediate energies, further measurements were made using the 1.4 GeV/ c magnetic spectrometer at TRIUMF at 200 and 400 MeV. The basic features of the spectrometer have been described previously.⁷

The targets were ${}^7\text{Li}$ enriched to 99.9% and used in the form of metal foils, one with an areal density of 92 mg/cm² and the other with 100 mg/cm². The solid angle of the spectrometer was determined by the use of the ${}^1\text{H}(p,p)$ reaction. Deuteron spectra taken at 200 and 400 MeV are shown in Figs. 1 and 2. The energy resolution of about 1 MeV full width at half maximum (FWHM) was sufficient to isolate reasonably well the ground states and the first excited state at 2.18 MeV. The cross sections were obtained by a

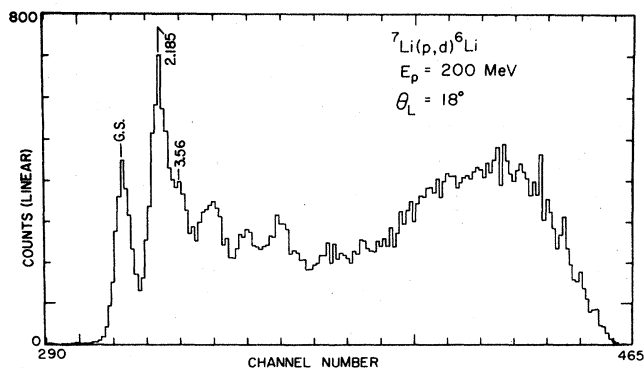


FIG. 1. Deuteron spectrum from the ${}^7\text{Li}(p,d){}^6\text{Li}$ reaction at an incident proton energy of 200 MeV and a laboratory scattering angle of 18° .

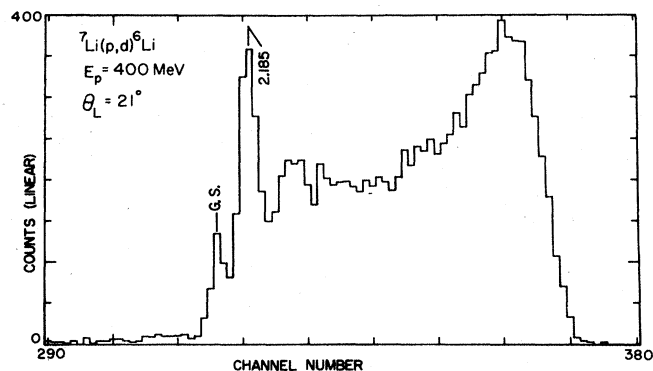


FIG. 2. Deuteron spectrum from the ${}^7\text{Li}(p,d){}^6\text{Li}$ reaction at an incident proton energy of 400 MeV and a laboratory scattering angle of 21° .

Gaussian decomposition of the region of interest in the spectra at the two energies. The resulting cross sections are shown in Fig. 3.

The data of others at 16.7, 33.6, 100, 156, 485, and 800 MeV are also shown in Fig. 3. The nature of the problem can be seen by noting that at 16.7 MeV the ground state transition is about two times as intense as the transition to the 3^+ state. As the projectile energy increases the cross section to the 3^+ state increases relative to the 1^+ state until at 100 MeV the ratio is about one, and at 800 MeV the 3^+ transition is about six times as intense as the ground state transition. The change in the ratio between 200 and 400 MeV can clearly be seen in Figs. 1 and 2 going from 200 to 400 MeV. Based upon the $1p$ -shell wave functions of Cohen and Kurath⁸ the predicted spectroscopic factor for the p -state transitions for the ground state transition is 0.72 and 0.55 for the 3^+ state.

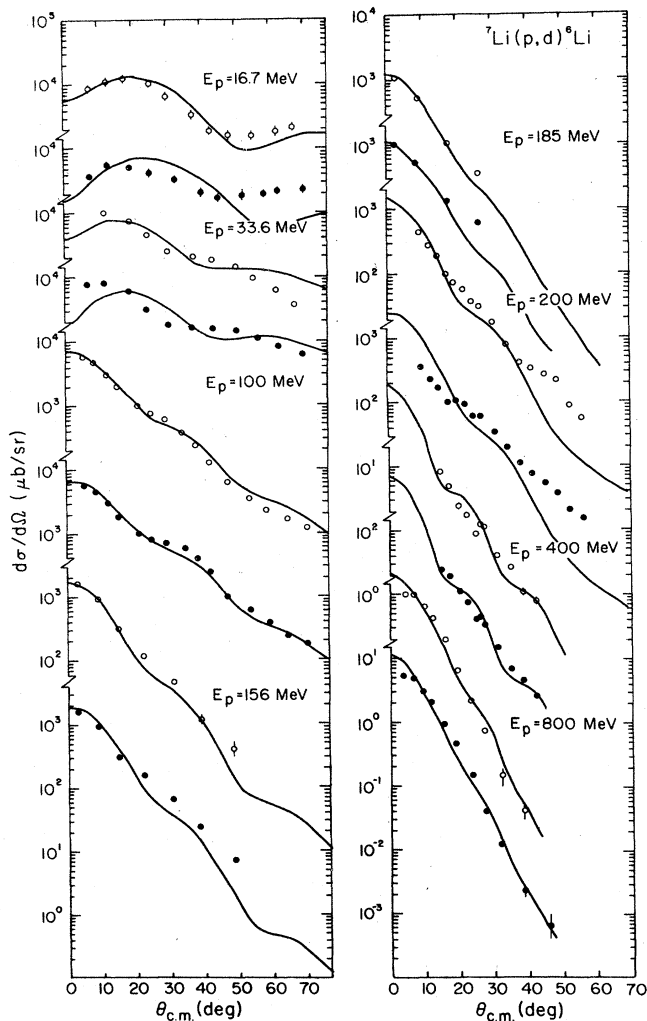


FIG. 3. Deuteron angular distributions for the ${}^7\text{Li}(p,d){}^6\text{Li}$ reaction to the 1^+ ground state (open circles) and 3^+ first excited state (closed circles). The solid lines are the results of DWBA calculations described in the text. The data shown at 16.7 MeV are from Ref. 1, 33.6 MeV (Ref. 2), 100 MeV (Ref. 3), 156 MeV (Ref. 4), 185 MeV (Ref. 5), and 800 MeV (Ref. 6), while the 200- and 400-MeV data are from the present work.

In order to determine the spectroscopic factors at the various energies, exact-finite range distorted wave calculations were carried out for all of the available data. The distorted wave Born approximation (DWBA) calculations were done using the code DWUCK5.⁹ The bound state was taken to have $r_0=1.25$ fm, $a_0=0.65$ fm, and the potential depth was determined by adjusting it to give the correct neutron separation energy. In addition, a Thomas factor of $\lambda=25$ was used in the bound state potential.

The code DWUCK5 allows for the inclusion of nonlocal effects by the introduction of a nonlocal correction parameter β . The values that were used at all energies were 0.85 for the incoming proton and the bound neutron, and 0.54 in the deuteron channel.

The proton optical potential parameters were taken from the literature¹⁰⁻¹⁷ and are shown in Table I. At the higher energies very little elastic scattering data exist for ${}^7\text{Li}$ and most of the potentials are based on ${}^{12}\text{C}$ data. Of particular use in this regard were the energy dependent ${}^{12}\text{C}$ potentials of Abdul-Jalil and Jackson.¹⁷ The deuteron optical potentials were based on the adiabatic deuteron approximation of Johnson and Soper.¹⁸ This was done in part because essentially no deuteron potentials were available on either ${}^7\text{Li}$ or ${}^{12}\text{C}$ for energies over 100 MeV, and in part because the adiabatic model compensates, to some degree, for deuteron breakup effects. The actual deuteron parameters were constructed according to the prescription of Harvey and Johnson¹⁹ and, since there are no neutron parameters available, the proton potentials at half of the value of E_p were doubled. The deuteron spin-orbit potential depth was taken to be the same as that of the proton at $E_p/2$. Table I shows the deuteron parameters for only those cases where the proton potentials at $E_p/2$ are not given.

A number of other potential parameter sets were used in the distorted wave calculations, but the sets listed in Table I gave the best overall description of the data and have some internal consistency. The results of the calculations are shown in Fig. 3. While the general description of the data is good and the slopes are reasonably well accounted for, there are details in the angular distributions at 200 MeV that are missed.

The experimental ratio of the cross sections for the excitation of the 3^+ state to the 1^+ state were obtained by taking the average of the ratios of the data at the various angles for each energy. The results are displayed in Fig. 4. The uncertainties shown are based on the standard deviations. The calculated (theoretical) ratios were obtained by taking the ratios of the DWUCK5 output $[\sigma(3^+)/\sigma(1^+)]_{\text{DW}}$ over the same angular range as the experimental data. The theoretical ratios were quite insensitive to the particular choice of optical potential parameters and to the geometrical parameters for the bound state. In fact, the value of $[\sigma(3^+)/\sigma(1^+)]_{\text{DW}}$ only varied between 0.74 at 16.7 MeV to 1.28 at 800 MeV. The ratio of the spectroscopic factors $C^2S(3^+)/C^2S(1^+)$ was then obtained as $[\sigma(3^+)/\sigma(1^+)]_{\text{exp}} \times [\sigma(1^+)/\sigma(3^+)]_{\text{DW}}$. The ratios of the spectroscopic factors are shown in Fig. 4 as the square points. To a good approximation these ratios are independent of the overall normalization of the experimental cross sections and the details of the distorted wave calculations. It should be noted that the variation of the ratios from about 0.6 at 16.7 MeV to about 4.4 at 800 MeV indicated a major breakdown of either the assumed reaction mechanism or the assumed wave functions for the states involved.

TABLE I. The optical model parameters used in the distorted wave calculations.

T (MeV) Channel	V_R (MeV)	r_R (fm)	a_R (fm)	V_I (MeV)	r_I (fm)	a_I (fm)	V_{SO} (MeV)	r_{SO} (fm)	a_{SO} (fm)	Ref.
1.67 p+ ⁷ Li	-48.3	1.15	0.4	*26.0 ^a	1.05	0.4	-22.0	1.20	0.4	10
16.7 d+ ⁶ Li	-74.4	1.47	0.89	*101.38	1.69	0.29	-9.8	1.56	0.28	11
33.0 p+ ⁷ Li	-50.2	1.21	0.61	*58.4	1.26	0.34	-19.6	1.17	0.32	11
100 p+ ⁷ Li	-25.6	1.02	0.65	-6.66	1.7	0.216	-25.9	1.02	0.65	12
100 d+ ⁷ Li	-73.4	1.21	0.59	-10.88	1.73	1.26	-9.8	1.0	0.53	13
156 p+ ⁷ Li	-12.84	1.4	0.515	-25.4	0.805	0.71	-7.36	0.915	0.453	14
156 d+ ⁶ Li	-50.88	1.13	0.53	*62.5	1.45	0.49	-1.44	1.86	0.4	15
185 p+ ⁷ Li	-27.3	0.938	0.571	-10.1	1.28	0.715	-16.24	0.938	0.571	16
185 d+ ⁶ Li	-40.0	1.10	0.71	-12.88	1.40	0.71	-19.64	1.10	0.697	16
200 p+ ⁷ Li	-12.5	1.2	0.63	-13.1	1.20	0.61	-16.4	0.9	0.47	17
400 p+ ⁷ Li	-9.98	0.948	0.472	-41.76	0.948	0.472	-15.0	0.948	0.472	17
800 p+ ⁷ Li	13.7	0.872	0.302	-68.93	0.948	0.472	-15.0	0.948	0.472	6

^aThe asterisk denotes a surface imaginary potential, while the others are volume potentials.

In order to test the importance of second order transitions via the inelastic channels we carried out calculations using the zero-range coupled channels code, CHUCK2.⁹ The inelastic excitations were calculated for a proton energy of 400 MeV using a simple model of ⁷Li, which assumes the states are members of a $K = \frac{1}{2}$ band. A deformation parameter of 0.80 was assumed.²⁰ The spectroscopic factors for the p -

state transfers were those of Cohen and Kurath,^{8,21} and the optical model parameters were those listed in Table I. The conventional multistep calculations for transitions to both the 1^+ and 3^+ states of ⁶Li differed by 5% or less from the standard single-step DWBA calculations. These results are consistent with earlier calculations carried out by others.⁶

Since the multistep processes did not adequately explain the ratio of the spectroscopic factors for the 1^+ and 3^+ states, other possibilities were explored. In particular, the effects of the addition of a small $1f_{7/2}$ component to the wave function for the bound state neutron was examined. In order to estimate the amount of f state in the ⁷Li target, we have used the finite-well Nilsson model²² for calculating the single-particle levels in a deformed nucleus. The parameters used for the radius are $r_0 = 1.25$ fm, for the diffusivity, $\alpha_0 = 0.65$ fm, and a spherical Thomas spin-orbit (SO) parameter, $\lambda = 25$. A quadrupole deformation parameter of $\beta_2 = 1.00$ gives a probability of 0.039 and 0.013 for the $f_{7/2}$ and $f_{5/2}$ states, respectively, in the lowest $j = 3/2$, $K = 1/2$ orbital.

The ratio of the spectroscopic factors for the f transition to the 3^+ and 1^+ states in ⁶Li can be estimated by using a simple LS coupling model. The f -state component in ⁷Li is assumed to consist of the state

$$\{[(p^2)_2 f]_{L=1} [(\frac{1}{2} \frac{1}{2})_1 \frac{1}{2}]_{1/2}\}_{J=3/2}$$

The transfer overlap of this wave function with the 1^+ state in ⁶Li is inhibited because of the 0.08 probability for the $[(p^2)_2 (\frac{1}{2} \frac{1}{2})_1]_{J=1}$ component. A further reduction results

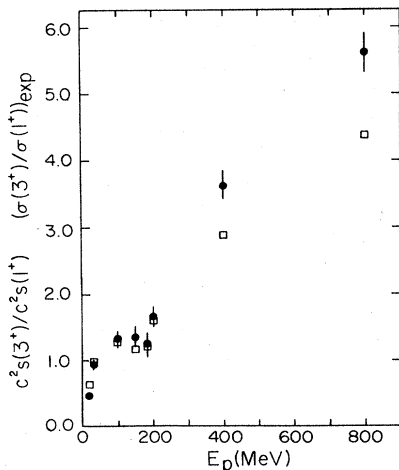


FIG. 4. The ratio of the experimental cross sections of the 3^+ state to the 1^+ ground state (solid circles) and the ratio of the spectroscopic factors to the same states (squares).

from the smaller $f_{5/2}$ transfer strength to the 1^+ state compared to the sum of $f_{7/2}$ and $f_{5/2}$ transfer strengths of the 3^+ state. As a result, the spectroscopic factor ratio for the f transfer is estimated to be $S_f(1^+)/S_f(3^+) \approx 0.04-0.06$. Hence, the f -state transfer goes primarily to the 3^+ state.

Exact-finite-range calculations were carried out with the same bound state and optical model parameters as discussed earlier. Various percentages of the results with a $1f_{7/2}$ wave function for the transferred neutron for the transition to the 3^+ state were combined incoherently with the cross sections for the $1p_{3/2}$ wave functions. The resulting ratios $[\sigma(3^+)/\sigma(1^+)]_{DW}$ were then used to calculate the ratio of spectroscopic factors. The ratios are shown in Fig. 5. The effects of adding a small amount of $1f_{7/2}$ to the wave function for the 3^+ transition are quite dramatic at the higher energies with very little effect at the lower energies. With an admixture of 15–20% $1f_{7/2}$, the spectroscopic factors are basically independent of energy from 16 to 800 MeV.

The coupled channels calculations were repeated for the 3^+ state with only a $1f_{7/2}$ neutron transfer. The $f_{7/2}$ spectroscopic factors were assumed to be proportional to the corresponding $p_{3/2}$ factors. The enhancement of the $f_{7/2}$ cross sections by the collective multistep effects was in the range of 30–40%. Thus, any estimate of the $f_{7/2}$ spectroscopic factor arrived at with a single-step calculation will have to be revised downward by this amount.

The method of taking experimental and theoretical ratios separately to calculate the ratio of spectroscopic factors has the disadvantage that it treats all points in the angular distribution equally. If one compares directly the shapes of the theoretical and experimental angular distributions to obtain spectroscopic factor ratios, values are found that are somewhat less than those obtained by taking the experimental and theoretical ratios separately. This occurs because the shapes of the experimental and theoretical angular distributions are not exactly the same and the smaller angle data are given greater weight in the comparison. For example, at 800 MeV the ratios of spectroscopic factors are 2.1 comparing shapes rather than 2.8 taking the points individually, for a 5% admixture of $f_{7/2}$ state.

In summary, the ${}^7\text{Li}(p,d){}^6\text{Li}$ reaction has been shown to be sensitive to high angular momentum components in the wave functions when the proton energies greater than about

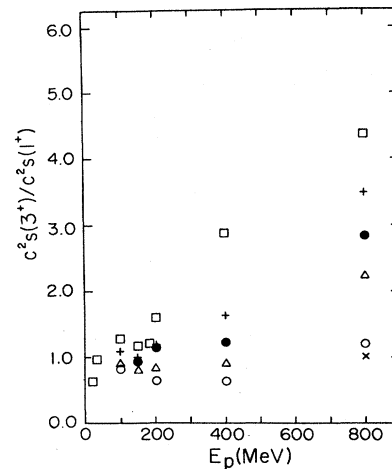


FIG. 5. The ratio of the spectroscopic factors for the 3^+ to the 1^+ states in ${}^6\text{Li}$ with various amounts of $l=3$ admixtures in the 3^+ transition. The squares are 0%, crosses are 3%, solid circles are 5%, triangles are 10%, open circles are 15%, and \times is 20%. For a 20% admixture only the ratio at 800 MeV is shown because the values at the other energies essentially coincided with the 15% values.

100 MeV are used. Explicitly, the increased population of the 3^+ in ${}^6\text{Li}$ relative to the 1^+ state, as the bombarding energy is increased to 800 MeV, can be understood in terms of small admixtures of $1f$ orbitals in the relevant states. These small admixtures are compatible with the finite-well Nilsson model. It is anticipated that high energy (p,d) data will be able to contribute to a more complete understanding of the nuclear wave function in other nuclei.

We are indebted to Professor J. R. Shepard for several helpful discussions of the theoretical aspects of this work, to Dr. R. M. Lombard for help in taking some of the data, and to W. Tew for his assistance in carrying out some of the distorted wave calculations. This work was supported in part by the U.S. Department of Energy, the Natural Sciences and Engineering Research Council of Canada, and the U.S. National Aeronautics and Space Administration.

*Present address: E. G. and G. Energy Measurements, Inc., Los Alamos, NM 87545.

†Present address: Laboratoire National Saturne, Centre d'Etudes Nucléaires Saclay, 91191 Gif-sur-Yvette Cedex, France.

¹W. G. Gulyamov *et al.*, *Izv. Akad. Nauk SSSR, Ser. Fiz.* **41**, 2214 (1977).

²L. A. Kull, *Phys. Rev.* **163**, 1066 (1967).

³J. K. P. Lee, S. K. Mark, P. M. Portner, and R. B. Moore, *Nucl. Phys.* **A106**, 357 (1968).

⁴D. Bachelier *et al.*, *Nucl. Phys.* **A126**, 60 (1969).

⁵B. Fagerström, J. Källne, O. Sundberg, and G. Tibell, *Phys. Scr.* **13**, 101 (1976).

⁶T. S. Bauer *et al.*, *Phys. Rev. C* **21**, 757 (1980); G. R. Smith *et al.*, *ibid.* **30**, 593 (1984).

⁷J. Källne *et al.*, *Phys. Rev. Lett.* **41**, 1638 (1978).

⁸S. Cohen and D. Kurath, *Nucl. Phys.* **A101**, 1 (1967).

⁹P. D. Kunz (unpublished).

¹⁰C. A. Pearson *et al.*, *Nucl. Phys.* **A191**, 1 (1972).

¹¹M. F. Werby, S. Edwards, and W. J. Thompson, *Nucl. Phys.* **A169**, 81 (1971).

¹²R. M. Haybron, *Nucl. Phys.* **A124**, 662 (1969).

¹³G. S. Mani, D. Jacques, and A. D. B. Dix, *Nucl. Phys.* **A165**, 145 (1971).

¹⁴V. Comparat *et al.*, *Nucl. Phys.* **A221**, 403 (1974).

¹⁵C. Rolland *et al.*, *Nucl. Phys.* **80**, 625 (1966).

¹⁶T. Sawada, *Nucl. Phys.* **74**, 289 (1965).

¹⁷I. Abdul-Jalil and D. F. Jackson, *J. Phys. G* **5**, 1699 (1979).

¹⁸R. C. Johnson and P. J. R. Soper, *Phys. Rev. C* **1**, 976 (1970).

¹⁹J. D. Harvey and R. C. Johnson, *Phys. Rev. C* **3**, 636 (1971).

²⁰S. A. Dickey, J. J. Kraushaar, and R. J. Peterson, *Z. Phys. A* **320**, 649 (1985).

²¹D. Kurath (private communication). We are indebted to Dr. Kurath for sending us the spectroscopic factors for transitions from the excited state of ${}^7\text{Li}$.

²²E. Rost, *Phys. Rev.* **154**, 994 (1967).